Viscoelastic characteristics of the canine cranial cruciate ligament complex at slow strain rates

Rosti Readioff [1], Brendan Geraghty [2], Ahmed Elsheikh [1, 3, 4] and Eithne Comerford [2, 5]

[1] School of Engineering, University of Liverpool, Liverpool, L69 3GH, UK.

[2] Institute of Life Course and Medical Sciences, University of Liverpool, William Henry Duncan Building, 6 West Derby Street, L7 8TX, UK.

[3] Beijing Advanced Innovation Center for Biomedical Engineering, Beihang University, Beijing, 100083, China.

[4] NIHR Moorfields BRC, 2/12 Wolfson Building, UCL Institute of Ophthalmology, 11-43 Bath Street, London, EC1V 9EL, UK

[5] School of Veterinary Science, Leahurst Campus, University of Liverpool, Chester High road, Neston, CH64 7TE, UK.

Corresponding Author:

Rosti Readioff[1]

School of Pharmacy and Bioengineering, Keele University, Staffordshire, ST4 7QB, UK.

E-mail address: r.readioff@keele.ac.uk

Abstract

Ligaments including the cruciate ligaments support and transfer loads between bones applied to the knee joint organ. The functions of these ligaments can get compromised due to changes to their viscoelastic material properties. Currently there are discrepancies in the literature on the viscoelastic characteristics of knee ligaments which are thought to be due to tissue variability and different testing protocols.

The aim of this study was to characterise the viscoelastic properties of healthy cranial cruciate ligaments (CCLs), from the canine knee (stifle) joint, with a focus on the toe region of the stress-strain properties where any alterations in the extracellular matrix which would affect viscoelastic properties would be seen.

Six paired CCLs, from skeletally mature and disease-free Staffordshire bull terrier stifle joints were retrieved as a femur-CCL-tibia complex and mechanically tested under uniaxial cyclic loading up to 10 N at three strain rates, namely 0.1, 1 and 10 %/min, to assess the viscoelastic property of strain rate dependency. The effect of strain history was also investigated by subjecting contralateral CCLs to an ascending (0.1, 1 and 10 %/min) or descending (10, 1 and 0.1 %/min) strain rate protocol.

The differences between strain rates were not statistically significant. However, hysteresis and recovery of ligament lengths showed some dependency on strain rate. Only hysteresis was affected by the test protocol and lower strain rates resulted in higher hysteresis and lower recovery. These findings could be explained by the slow process of uncrimping of collagen fibres and the contribution of proteoglycans in the ligament extracellular matrix to intra-fibrillar gliding, which results in more tissue elongations and higher energy dissipation.

This study further expands our understanding of canine CCL behaviour, providing data for material models of femur-CCL-tibia complexes, and demonstrating the challenges for engineering complex biomaterials such as knee joint ligaments.

Introduction

Ligaments play a major role in stifle (knee) joint stability (Budras, 2007; Levangie and Norkin, 2005), with part of the primary support being provided by the cranial cruciate ligament (CCL) (Carpenter and Cooper, 2000; Slatter, 2002). The CCL is the most commonly ruptured canine stifle joint ligament (CCLR) (Arnoczky, 1988; Gianotti et al., 2009) following acute injury or chronic disease, which can lead to destabilisation of surrounding structures and the subsequent development of osteoarthritis (Arnoczky, 1988; Bennett et al., 1988; Brooks, 2002; Comerford et al., 2006). There is a large economic cost associated with managing canine CCLR, for example in the United States alone the economic cost was estimated to be at least one billion dollars in 2003 (Wilke et al., 2005). Both human and canine CCL failure significantly increases the incidence of age-associated joint degeneration (Lee et al., 2014; Liu et al., 2003; Peters et al., 2018) and so understanding the tissue's fundamental material properties can assist with the prediction and effective management of ligament injuries.

The phenomenon of viscoelastic characteristics including strain rate dependency, hysteresis, creep and stress relaxation has been observed consistently in soft biological tissues such as the sclera (Elsheikh et al., 2010; Geraghty et al., 2020), cornea (Elsheikh et al., 2011; Kazaili et al., 2019), and tendon (Robinson et al., 2004; Zuskov et al., 2020). Similarly, ligaments inherit non-linear viscoelastic characteristics exhibiting both elastic and viscous behaviour, hence they are history- and time-dependent (Bonner et al., 2015; Fung, 1993; Ristaniemi et al., 2018). The initial part of the non-linear load-deformation behaviour in ligaments is the toe region where the wavy collagen fibres become taut and straighten as load is applied, hence the crimp is removed (Fratzl et al., 1998). In this zone, there is a relatively large deformation of the tissue with little increase in load and this permits initial joint deformations

with minimal tissue resistance (Dale and Baer, 1974; Fratzl et al., 1998; Wingfield et al., 2000).

Several studies tested for material characteristics of knee joint ligaments at traumatic loading rates and to failure loads (Crisco et al., 2002; Crowninshield and Pope, 1976; Lydon et al., 1995). The loading rate is reported to be directly proportional to the tension which develops in ligaments (Pioletti et al., 1999; Woo et al., 1990b). This characteristic was also evident in a study investigating lower strain rates between approximately 2 and 54 %/min representing physiological conditions other than trauma (Haut and Little, 1969). The study reported no change in the overall shape of the stress-strain curve, however, rapid change in the tangent modulus was found with the slow strain rates (between 1.7 and 10.8 %/min) and the change became progressively smaller with higher strain rates (above 10.8 %/min). Similarly, it was reported that strain rate dependency decreases with the increase of deformation rate (Bonner et al., 2015; Crisco et al., 2002). The stress-strain behaviour in the toe region (6% strain) showed strain rate dependency in canine CCL (Haut and Little, 1969). However, a study on rabbit medial collateral ligament complexes at varying strain rates (between 0.66 and 9300 %/min) showed that the ligaments were only minimally strain rate dependent (Woo et al., 1990b, 1981). The small effect of strain rate stiffening could be because the studies combined stress-strain characteristics at the toe region with the elastic region (Haut and Little, 1969; Ristaniemi et al., 2018).

During high strain rates, hysteresis (energy dissipated) in the ligament may protect the tissue from injury (Bonifasi-Lista et al., 2005). However, there are contradicting findings about hysteresis in soft biological tissues in relation to strain rates. Initially, hysteresis was believed to be weakly dependent on strain rates (Fung, 1993). In contrary, a study on the viscoelastic tensile response of bovine cornea showed an increase in hysteresis with decreasing strain rates (Boyce et al., 2007). It is suggested that Fung's belief in this phenomenon was based on

a small number of experiments on rabbit papillary muscle using only three different strain rates (Haslach, 2005). Hence, Fung's findings only approximately support the independence of hysteresis from strain rates.

Therefore, there is a lack of understanding on the strain rate dependency and hysteresis of canine CCLs. Current information is limited to no clear methodological investigations on the strain rate dependency and hysteresis of the CCLs at the toe region (the initial part of non-linear load-deformation behaviour) where collagen fibres tighten and uncrimps with applied load, and importantly, any alterations in the extracellular matrix will be observed (Comerford et al., 2014; Lujan et al., 2009). Therefore, the purpose of this study was to characterise the viscoelastic properties of healthy canine CCLs as a femur-CCL-tibia complex, with a focus on the toe region of the stress-strain properties. This quantification is important when comparing the mechanical characteristics of the CCL and when developing synthetic, auto and allo-grafts to be used in future therapies for ligament replacement.

Materials & Methods

Cranial cruciate ligament storage and preparation

Cadaveric disease-free canine stifle joint pairs from skeletally mature Staffordshire bull terriers (n=6 pairs) euthanatized for reasons other than musculoskeletal injury were obtained with full ethical permission from the Veterinary Research Ethics Committee ((VREC65), Institute of Veterinary Science, University of Liverpool). Inclusion criteria for cadaveric samples were a bodyweight >15kg and age between 1.5 and 5 years old. The entire stifle joints were frozen at -20°C until required and defrosted at room temperature prior to removing the CCLs as a femur-CCL-tibia complex (Readioff, 2017; Readioff et al., 2020). In order to harvest the femur-CCL-tibia complex, initially the stifle joints were dissected.

Subsequently, approximately 10 mm of the femoral and tibial bones were left connected to the CCLs which allowed for the measurement of end-to-end ligament deformation as well as helping to facilitate the clamping of the specimen (Fig. 1).

The extracted femur-CCL-tibia complexes were maintained in a moistened state in paper towels soaked with phosphate buffered saline (PBS; Sigma, Poole, UK) and frozen at -80°C until they were required for testing (Woo et al., 1986). Prior to testing, the samples were thawed at room temperature and two 1.1 mm arthrodesis wires (Veterinary Instrumentation, Sheffield, UK) were drilled through the tibial and femoral bone ends (Fig. 1). These pins were placed to provide extra grip as well as to replicate the ligament's slight proximal-to-distal outward spiral when secured using custom built steel clamps (Arnoczky, 1983; Arnoczky and Marshall, 1977). The ducktail clamps were designed to provide a secure grip as well as ensuring that the CCLs were free and unobstructed throughout the experiment (Fig. 2). The clamped samples were then mounted on a mechanical testing machine.

Cranial cruciate ligament length

A modified version of a previously described method was used to determine the average length of CCL from the craniomedial and caudolateral portions of a ligament (Comerford et al., 2005; Vasseur et al., 1991). In this study, measurements between the insertion and origin of the CCLs at the cranial and caudal planes, as well as the lateral and medial planes were taken using a Vernier callipers (D00352, Duratool, Taiwan) accurate to ±10 µm. The mean values of these four length measurements were recorded to give an accurate record of the length of the CCL before deformation (Supplementary Materials (Fig. S1)).

Cranial cruciate ligament cross-sectional area

The method by Goodship and Birch was used to measure cross sectional area (CSA) of the CCLs (Goodship and Birch, 2005). In brief, alginate dental impression paste (UnoDent, UnoDent Ltd., UK) was used to make a mould around the CCL. Once set, the mould was removed from the CCL and was used to create replicas of the CCLs. The replicas were cut into two in the middle and the surface of the replicas showing middle CSA were estimated using ImageJ (a public domain Java image processing program) (Supplementary Materials (Fig. S2)).

Mechanical testing

An Instron 3366 materials testing machine (Instron, Norwood, MA) fitted with a 10 N load cell (Instron 2530-428 with ±0.025 N accuracy) was used to perform tensile tests. Initially, a preload of 0.1 N was applied to remove laxity within the CCL (Provenzano et al., 2002). Application of the preload was then followed by preconditioning the CCLs to ensure that they were in a steady state and would produce comparable and reproducible load-elongation curves (Butler et al., 1978; Fung, 1993; Savelberg et al., 1993). Preconditioning involved performing ten loading-unloading cycles up to a maximum load of 10 N at 10 %/min strain rate (Ebrahimi et al., 2019; Woo et al., 1991). Subsequently the CCL was subjected to cyclic tensile loading-unloading tests investigating stress-strain behaviour of the ligament at the toe region through the application of 10 N load at sequential slow strain rates of 0.1, 1 and 10 %/min. Each strain rate consisted of three loading-unloading cycles which allowed for reproducible results. Between each two cycles, including the preconditioning procedure, a period of six minutes recovery time was given (Ebrahimi et al., 2019; Viidik, 1968). From the paired stifle joints, the left CCLs were exposed to an ascending strain rate test in which the rate of strain was increased from 0.1 to 1 and to 10 %/min and the right CCLs were exposed

to a descending strain rate in which the CCL was tested under decreasing strain rates from 10 to 1 and to 0.1 %/min (Pioletti et al., 1999; Pioletti and Rakotomanana, 2000). A slow speed was chosen to better observe tissue response to loading at the toe region of load-deformation curves. The reverse orders of strain rate tests (ascending and descending strain rates tests) were carried out to identify characteristics associated with strain history of the ligaments at the toe region.

Data Analysis

All analyses on the collected load-deformation data were performed using Excel spreadsheets (Microsoft Office 2010, US) and graphs were plotted using MATLAB (MATLAB R2020a) (code for the graphs can be found in the Supplementary Materials). Nominal stress and strain values were estimated following Equations 1 and 2 (Haut and Little, 1969; Woo et al., 1981) and from these stress and strain values, tangent modulus values were determined (Equation 3). Numerical integrations were used to estimate hysteresis which is defined by the area between loading and unloading stress-strain curves (Elsheikh et al., 2008). In addition, ligament extension before and after recovery were studied to investigate strain history and strain rate dependencies as a result of applying loads at different strain rate orders (loading at ascending or descending rates).

$$\sigma = \frac{F}{CSA} \qquad \text{Equation 1}$$

where σ is stress in MPa, F is applied load in N and CSA is cross-sectional area at the middle of the CCL in mm^2.

$$\varepsilon = \frac{\Delta L}{L_0}$$ Equation 2

where ε is strain, ΔL is change in length in mm ($\Delta L = L_0 - L_1$), L_0 is initial length and L_1 is deformed length of the CCL in mm.

$$E_{tan} = \frac{\delta \sigma}{\delta \varepsilon}$$ Equation 3

where E_{tan} is tangent modulus in MPa.

Statistical Analysis

CCL lengths measured at different planes were categorised into cranial, caudal, medial and lateral groups. Statistical tests were performed using one-way analysis of variance (ANOVA) followed by a Bonferroni post-hoc test for multiple comparisons.

A two-tailed t-test (two samples with unequal variance) was used to test for differences between results obtained from the ascending and descending strain rate tests. In addition, one-way ANOVA followed by a Bonferroni post-hoc test for multiple comparisons was performed to test dependencies of tensile responses of the ligaments on strain rates. Distribution of data was illustrated in boxplots and suspected outliers were defined as any value greater than or equal to 1.5 times the interquartile range (range between the first and third quartiles).

All statistical analyses were performed in Microsoft Office Excel and 95% confidence level ($p < 0.05$) was selected to define significance for all statistical tests.

198

199 ## Results

200 *Cranial cruciate ligament samples*

201 The CCL samples (n=6 paired stifle joints) used to investigate mechanical properties of the
202 ligament were of mixed gender (female=3 and male=3) and the bodyweight of the cadavers
203 were in the range of 17 to 25.5 kg (20.68 ± 3.85 kg).

204

205 *Cranial cruciate ligament length*

206 The lengths of the CCLs at different planes were in the range of 7.88 to 23.16 mm and the
207 measurements at different planes of the individual ligaments are reported in Table 1.

208 The ANOVA test showed statistically significant results in measuring CCL length in different
209 plane views. The analysis showed that length measurements recorded at different planes were
210 statistically different except for comparisons between medial and lateral planes
211 (Supplementary Material (Table 1)).

212

213 *Cranial cruciate ligament cross-sectional area*

214 The cross-sectional areas of the CCLs were in the range of 11.09 to 23.62 mm^2 (16.1 ± 5.1
215 mm^2) and cross-sectional areas of individual ligaments are reported in Table 2.

216

217 *Mechanical properties*

218 Stress-strain

219 The stress-strain curves at 0.1, 1 and 10 %/min strain rates conformed to the typical non-
220 linear behaviour as expected in canine CCLs (Haut and Little, 1969) (Fig. 3a). The stress-
221 strain curves illustrated an increase in stress with increasing strain, and similarly an increase
222 in stiffness was observed with increasing strain rates (Fig. 3b). Although there was a small
223 increase in stress with increasing strain rates, the increase was not statistically significant.

224 The stress responses of the ligaments during ascending test protocol, where the cyclic loading
225 commenced with 0.1 %/min then increased to 1 %/min and finally to 10 %/min, were similar
226 to responses during descending test protocol (the reverse of ascending test protocol). The
227 stress-strain curves show that there are minimal differences in stress values between the two
228 test protocols below 3% strain, and these differences become more distinguishable above 3%
229 strain (Fig. 4a, b and c). The testing protocols only minimally affected the stress-strain
230 characteristics and not statistically significant. There are notably different mechanical
231 behaviours among the specimens, as indicated by the grey dots in Fig. 4a, b and c, and not all
232 specimens reached 5% strain (Supplementary Materials (Fig. S3, S4 and S5).

233

234 Tangent modulus-stress

235 Tangent modulus (E_t), indicating the stiffness behaviour of the CCLs, increased with
236 increasing stress (Fig. 3b) in both ascending and descending testing protocols. Similar to the
237 observations from the stress-strain curves, the tangent modulus-stress lines between the two
238 testing protocols (ascending and descending) were only minimally different and not
239 statistically significant. Although not statistically significant, the increase in tangent modulus
240 with strain rates was notable at higher stress values (Fig. 4d, e and f). For example, at 0.5
241 MPa stress, average tangent modulus values from the ascending test protocol were 26.62,
242 31.40 and 32.66 MPa during loading at 0.1, 1 and 10 %/min strain rates.

Hysteresis

The results of this study show that hysteresis or dissipated energy are statistically different between the ascending and descending testing protocols ($p= 0.0043$). The mean values for hysteresis at 0.1, 1 and 10 %/min strain rates were 0.0032 (cycle 13), 0.0020 (cycle 16) and 0.0016 (cycle 19) MPa in ascending and 0.0040 (cycle 19), 0.0042 (cycle 16) and 0.0037 (cycle 13) MPa in descending testing protocol (Fig. 5a). The dissipated energy decrease from the first preconditioning cycle to the tenth (last) cycle was 85% for both testing protocols. In addition, hysteresis decreased with increasing strain rates (Fig. 5b). This characteristic was statistically significant during the ascending testing protocol ($p= 0.039$ between 0.1 and 1 %/min, and $p= 0.013$ between 0.1 and 10 %/min).

Recovery

Length of the CCLs before and after the recovery period between each cycle showed consistent values during preconditioning and these values were in the range of 0.095 to 0.078 mm during ascending and 0.124 to 0.095 mm during descending tests (Fig. 6a). Unlike hysteresis, statistical analysis showed that tissue recovery was not different during ascending and descending tests. However, tissue length recovery was strain rate dependent and statistical analysis showed differences in recovery between 0.1 and 1 %/min ($p= 0.018$), and 0.1 and 10 %/min ($p= 0.001$) (Fig. 6b).

Discussion

The aim of this study was to gain a greater understanding of the viscoelastic behaviour of the canine CCLs as a femur-CCL-tibia complex at the toe region of the stress-strain curves in order to better mechanically detail the material for its use in developing future therapies. Therefore, we carried out an experimental study investigating the nonlinear viscoelastic properties of CCLs, namely strain rate dependency, hysteresis and recovery, from healthy canine stifle joints. The findings in this study are the first to report the slow strain rate dependency of the canine cruciate ligament across three orders of magnitude with ascending and descending test arrangements. A previous study showed that with high strain rates, the toe region of stress-strain curves appears at lower strain levels (Haut and Little, 1969), however in order to study the toe region in detail without being limited to the level of strain, slow strain rates (≤10 %/min) were utilised during mechanical tests in the current study.

The non-linear stress-strain pattern for the CCLs is consistent to that previously reported in studies on biological tissues such as tendons and ligaments (Bonner et al., 2015; Crisco et al., 2002; Haut and Little, 1969; Pioletti et al., 1999; Pioletti and Rakotomanana, 2000). The stress-strain and tangent modulus-stress characteristics of the CCLs were similar during the ascending and descending testing protocols (Fig. 3 and 4). These findings are similar to a previous study on bovine anterior cruciate ligament-bone complex where specimens were loaded up to 300 N at seven different strain rates (6, 60, 300, 600, 1200, 1800 and 2400 %/min) and then tested for strain rate order by reloading the ligaments at the 6 and 300 %/min strain rates (Pioletti et al., 1999). They found identical stress-strain behaviour for the initial and reloaded specimens suggesting no difference in changing test protocols via strain rate orders. Their study applied higher strain rates (6-2400 %/min) than those used in the current paper and they reloaded the tissue in an ascending strain rate order only. Pioletti et al. did not study tissue hysteresis or recovery, but they reported increases in linear tangent

289 moduli with increasing strain rates (although not statistically significant) which is similar to
290 the findings in the current study.

291 The mechanical response of human knee ligaments to loading depends on strain rate which is
292 less pronounced at lower rates (Dorlot et al., 1980; van Dommelen et al., 2005) and this was
293 also observed in the current study. It is believed that during lower strain rates the collagen
294 fibrils in patella tendons undergo significantly less recruitment (Clemmer et al., 2010) and
295 this could potentially be similar in the case of the CCLs. At slow strain rates (≤10 %/min) the
296 collagen fibrils uncrimp with applied load and then show intra-fibrillar gliding (Bonner et al.,
297 2015; Karunaratne et al., 2018). However, at fast strain rates (≥300 %/min) fibrils go from an
298 unloaded state directly to intra-fibrillar gliding where the matrix bond between the collagen
299 molecules are broken before the removal of collagen crimps (Bonner et al., 2015). This could
300 mean that the extracellular matrix components such as proteoglycans, which is directly linked
301 to the mechanics of ligaments during uncrimping of the collagen fibres, might not affect the
302 mechanical response during loads at higher strain rates.

303 In our study, hysteresis, which represents the dissipation of energy within the tissue, has
304 shown some dependencies on strain rates and decreases with increasing strain rates (Fig. 5b).
305 This finding contradicts the conclusions from previous literature (Bonifasi-Lista et al., 2005;
306 Woo et al., 1981) but agrees with a recent study on tendon fascicle mechanics (Rosario and
307 Roberts, 2020) and a study on bovine cornea (Boyce et al., 2007) which found a decrease in
308 strain energy storage with increased loading rate. The discrepancies in results might be due to
309 following different testing protocols, in particular the rate of applied loads. In the current
310 study, where slow strain rates of ≤10 %/min were used, the tissue goes through more steps
311 (uncrimping collagen fibres, intra-fibrillar gliding and then loading of collagen respectively

with applied loads) during lower strain rates (Bonner et al., 2015), and this slow process results in more tissue elongations hence higher energy dissipation.

The CCLs showed higher length recovery during higher strain rates compared to the lower strain rates (Fig. 6). This behaviour could be a result of resilience in the fascicular level of the tissue. It has been reported that during slow strain rates, the resilience in the fascicular level is lowest (Rosario and Roberts, 2020) which could lead to higher changes in the microstructural organisation of the tissue. Hence, the tissue's length might not fully recover within the same recovery time as during higher strain rate tests. However, it is important to note that although the higher strain rate might seem to result in a more recovered ligament length, it is possible that the tissue collagen fibres are still crimping back as a result of previous loading history or insufficient recovery time. Further study in this area especially at the microstructural level of knee ligaments is necessary to better understand the effects of loading rates on the organisations of the fibres and extracellular matrix.

There were several limitations to our study. Preparing specimens for mechanical tests as a whole unit (femur-CCL-tibia complex) might have introduced some limitations such as overlooking the complexity of the anatomical structure of the CCLs which consists of two fibre bundles (caudolateral (CLB) and craniomedial bands (CMB)) functioning independently from one another in stifle joint flexion and extension (Arnoczky and Marshall, 1977; Carpenter and Cooper, 2000). Independent functioning of the CLB and the CMB allows the fibre bundles to reach their maximum potential (Arnoczky and Marshall, 1977; Carpenter and Cooper, 2000; Tanegashima et al., 2019). However, it is important to note that these two fibre bundles are not structurally segregated within the tissue, thus allowing the ligament to function as a united structure (Heffron and Campbell, 1978). In addition, the approximation methods adopted to measure the cross-sectional area and length of the specimens might be

considered as another limitation. Further investigation with a larger number of specimens might improve the reliability of the statistical analysis and provide a broader view on the effect of cadaveric demography (i.e. age, gender, bodyweight) on the mechanical properties and microstructural organisations of knee ligaments (Duval et al., 1999; Woo et al., 1990a, 1990b).

Conclusions

The current study focused on the viscoelastic behaviour, such as strain rate dependency, hysteresis and recovery of canine CCLs at slow strain rates to better understand the tissue behaviour at the toe region where the constituents of the extracellular matrix makes a major contribution to ligament mechanics.

Our changing test protocols via strain rate orders only affected hysteresis which might be a result of the strain history of the tissue or high-level of biological variability across samples. The stress-strain of the CCLs at the toe-region associated with the extracellular matrix of the ligaments was not strain rate dependent. However, hysteresis and recovery were strain rate dependent and this is likely due to changes in microstructural organisation of the ligaments during mechanical tests.

The result of our study indicates the need for further investigations on the viscoelastic behaviour of the canine CCLs when loaded with different orders of strain rates, with a focus on extracellular matrix and collagen fibre organisations.

Acknowledgments

We thank Mr. Lee Moore, Mr. Ben Jones and the staff at Veterinary Teaching Suite, School of Veterinary Science for their assistance during sample collection. We also thank Mr. John Curran at School of Engineering, University of Liverpool, for their assistance during manufacturing parts of the experimental setup.

References

Arnoczky, S.P., 1988. The cruciate ligaments: The enigma of the canine stifle. J. Small Anim. Pract. 29, 71–90. https://doi.org/DOI 10.1111/j.1748-5827.1988.tb02267.x

Arnoczky, S.P., 1983. Anatomy of the anterior cruciate ligament. Clin. Orthop.

Arnoczky, S.P., Marshall, J.L., 1977. The cruciate ligaments of the canine stifle: An anatomical and functional analysis. Am. J. Vet. Res. 38, 1807–1814.

Bennett, D., Tennant, B., Lewis, D.G., Baughan, J., May, C., Carter, S., 1988. A reappraisal of anterior cruciate ligament disease in the dog. J. Small Anim. Pract. 29, 275–297. https://doi.org/DOI 10.1111/j.1748-5827.1988.tb02286.x

Bonifasi-Lista, C., Lake, S.P., Small, M.S., Weiss, J.A., 2005. Viscoelastic properties of the human medial collateral ligament under longitudinal, transverse and shear loading. J Orthop Res. https://doi.org/10.1016/j.orthres.2004.06.002

Bonner, T.J., Newell, N., Karunaratne, A., Pullen, A.D., Amis, A.A., A, M.J.B., Masouros, S.D., 2015. Strain-rate sensitivity of the lateral collateral ligament of the knee. J. Mech. Behav. Biomed. Mater.

Boyce, B.L., Jones, R.E., Nguyen, T.D., Grazier, J.M., 2007. Stress-controlled viscoelastic tensile response of bovine cornea. J. Biomech. 40, 2367–2376. https://doi.org/DOI 10.1016/j.jbiomech.2006.12.001

381 Brooks, P.M., 2002. Impact of osteoarthritis on individuals and society: How much
382 disability? Social consequences and health economic implications. Curr. Opin.
383 Rheumatol. https://doi.org/10.1097/00002281-200209000-00017
384 Budras, K.-D., 2007. Anatomy of the dog, 5th ed, Vet series. Schlu□tersche, Hannover.
385 Butler, D.L., Noyes, F.R., Grood, E.S., 1978. Measurement of the mechanical properties of
386 ligaments, in: CRC Handbook of Engineering in Medicine and Biology Section B:
387 Instruments and Measurements. CRC Press Inc., West Palm Beach, pp. 279–314.
388 Carpenter, D.H., Cooper, R.C., 2000. Mini review of canine stifle joint anatomy. Anat.
389 Histol. Embryol. 29, 321–329. https://doi.org/DOI 10.1046/j.1439-0264.2000.00289.x
390 Clemmer, J., Liao, J., Davis, D., Horstemeyer, M.F., Williams, L.N., 2010. A mechanistic
391 study for strain rate sensitivity of rabbit patellar tendon. J. Biomech. 43, 2785–2791.
392 https://doi.org/10.1016/j.jbiomech.2010.06.009
393 Comerford, E.J., Geraghty, B., Hama Rashid, R., Elsheikh, A., 2014. The Contribution of
394 Proteoglycans to the Viscoelasticity of the Canine Anterior Cruciate Ligament.
395 Osteoarthritis Cartilage.
396 Comerford, E.J., Tarlton, J.F., Innes, J.F., Johnson, K.A., Amis, A.A., Bailey, A.J., 2005.
397 Metabolism and composition of the canine anterior cruciate ligament relate to
398 differences in knee joint mechanics and predisposition to ligament rupture. J. Orthop.
399 Res. 23, 61–66. https://doi.org/10.1016/j.orthres.2004.05.016
400 Comerford, E.J., Tarlton, J.F., Wales, A., Bailey, A.J., Innes, J.F., 2006. Ultrastructural
401 differences in cranial cruciate ligaments from dogs of two breeds with a differing
402 predisposition to ligament degeneration and rupture. J Comp Pathol.
403 https://doi.org/10.1016/j.jcpa.2005.06.004
404 Crisco, J.J., Moore, D.C., McGovern, R.D., 2002. Strain-rate sensitivity of the rabbit MCL
405 diminishes at traumatic loading rates. J. Biomech. 35, 1379–1385.

406 Crowninshield, R.D., Pope, M.H., 1976. The strength and failure characteristics of rat medial
407 collateral ligaments. J. Trauma 16, 99–105.
408 Dale, W.C., Baer, E., 1974. Fiber-buckling in composite systems: A model for ultrastructure
409 of uncalcified collagen tissues. J. Mater. Sci. 9, 369–382. https://doi.org/Doi
410 10.1007/Bf00737836
411 Dorlot, J.M., Ait Ba Sidi, M., Tremblay, G.M., Drouin, G., 1980. Load elongation behavior
412 of the canine anterior cruciate ligament. J. Biomech. Eng.
413 https://doi.org/10.1115/1.3149572
414 Duval, J.M., Budsberg, S.C., Flo, G.L., Sammarco, J.L., 1999. Breed, sex, and body weight
415 as risk factors for rupture of the cranial cruciate ligament in young dogs. J. Am. Vet.
416 Med. Assoc. 215, 811–814.
417 Ebrahimi, M., Mohammadi, A., Ristaniemi, A., Stenroth, L., Korhonen, R.K., 2019. The
418 effect of different preconditioning protocols on repeatability of bovine ACL stress-
419 relaxation response in tension. J. Mech. Behav. Biomed. Mater. 90, 493–501.
420 https://doi.org/10.1016/j.jmbbm.2018.10.041
421 Elsheikh, A., Geraghty, B., Alhasso, D., Knappett, J., Campanelli, M., Rama, P., 2010.
422 Regional variation in the biomechanical properties of the human sclera. Exp. Eye Res.
423 90, 233–624. https://doi.org/10.1016/j.exer.2010.02.010
424 Elsheikh, A., Kassem, W., Jones, S.W., 2011. Strain-rate sensitivity of porcine and ovine
425 corneas. Acta Bioeng. Biomech. 13, 25–36.
426 Elsheikh, A., Wang, D., Rama, P., Campanelli, M., Garway-Heath, D., 2008. Experimental
427 assessment of human corneal hysteresis. Curr. Eye Res. 33, 205–213.
428 https://doi.org/10.1080/02713680701882519

429 Fratzl, P., Misof, K., Zizak, I., Rapp, G., Amenitsch, H., Bernstorff, S., 1998. Fibrillar
430 structure and mechanical properties of collagen. J. Struct. Biol. 122, 119–122.
431 https://doi.org/DOI 10.1006/jsbi.1998.3966
432 Fung, Y.C., 1993. Biomechanics: Mechanical properties of living tissues, 2nd ed. Springer,
433 New York.
434 Geraghty, B., Abass, A., Eliasy, A., Jones, S.W., Rama, P., Kassem, W., Akhtar, R.,
435 Elsheikh, A., 2020. Inflation experiments and inverse finite element modelling of
436 posterior human sclera. J. Biomech. 98, 109438.
437 https://doi.org/10.1016/j.jbiomech.2019.109438
438 Gianotti, S.M., Marshall, S.W., Hume, P.A., Bunt, L., 2009. Incidence of anterior cruciate
439 ligament injury and other knee ligament injuries: A national population-based study.
440 J. Sci. Med. Sport 12, 622–627. https://doi.org/10.1016/j.jsams.2008.07.005
441 Goodship, A.E., Birch, H.L., 2005. Cross sectional area measurement of tendon and ligament
442 in vitro: a simple, rapid, non-destructive technique. J. Biomech. 38, 605–608.
443 https://doi.org/DOI 10.1016/j.jbiomech.2004.05.003
444 Haslach, H.W., 2005. Nonlinear viscoelastic, thermodynamically consistent, models for
445 biological soft tissue. Biomech. Model. Mechanobiol. 3, 172–189.
446 https://doi.org/10.1007/s10237-004-0055-6
447 Haut, R.C., Little, R.W., 1969. Rheological properties of canine anterior cruciate ligaments.
448 J. Biomech. 2, 289–298. https://doi.org/Doi 10.1016/0021-9290(69)90085-2
449 Heffron, L.E., Campbell, J.R., 1978. Morphology, histology and functional anatomy of the
450 canine cranial cruciate ligament. Vet. Rec.
451 Karunaratne, A., Li, S., Bull, A.M.J., 2018. Nano-scale mechanisms explain the stiffening
452 and strengthening of ligament tissue with increasing strain rate. Sci. Rep.
453 https://doi.org/10.1038/s41598-018-21786-z

454 Kazaili, A., Geraghty, B., Akhtar, R., 2019. Microscale assessment of corneal viscoelastic
455 properties under physiological pressures. J. Mech. Behav. Biomed. Mater. 100,
456 103375. https://doi.org/10.1016/j.jmbbm.2019.103375
457 Lee, K., Williamson, K., Clegg, P., Comerford, E., Canty-Laird, E., 2014. The stem cell niche
458 in tendon and ligament: investigating alterations with ageing and disease, in: British
459 Journal of Sports Medicine. BMJ, pp. A35–A36. https://doi.org/10.1136/bjsports-
460 2014-094114.54
461 Levangie, P.K., Norkin, C.C., 2005. Joint structure and function: A comprehensive analysis,
462 4th ed. F.A. Davis Co., Philadelphia.
463 Liu, W.H., Burton-Wurster, N., Glant, T.T., Tashman, S., Sumner, D.R., Kamath, R.V., Lust,
464 G., Kimura, J.H., Cs-Szabo, G., 2003. Spontaneous and experimental osteoarthritis in
465 dog: similarities and differences in proteoglycan levels. J. Orthop. Res.
466 https://doi.org/Doi 10.1016/S0736-0266(03)00002-0
467 Lujan, T.J., Underwood, C.J., Jacobs, N.T., Weiss, J.A., 2009. Contribution of
468 glycosaminoglycans to viscoelastic tensile behavior of human ligament. J. Appl.
469 Physiol. https://doi.org/10.1152/japplphysiol.90748.2008
470 Lydon, C., Crisco, J.J., Panjabi, M., Galloway, M., 1995. Effect of elongation rate on the
471 failure properties of the rabbit anterior cruciate ligament. Clin. Biomech. 10, 428–433.
472 Peters, A.E., Akhtar, R., Comerford, E.J., Bates, K.T., 2018. The effect of ageing and
473 osteoarthritis on the mechanical properties of cartilage and bone in the human knee
474 joint. Sci. Rep. 8, 5931. https://doi.org/10.1038/s41598-018-24258-6
475 Pioletti, D.P., Rakotomanana, L.R., 2000. Non-linear viscoelastic laws for soft biological
476 tissues. Eur. J. Mech. - ASolids 19, 749–759. https://doi.org/Doi 10.1016/S0997-
477 7538(00)00202-3

478 Pioletti, D.P., Rakotomanana, L.R., Leyvraz, P.F., 1999. Strain rate effect on the mechanical
479 behavior of the anterior cruciate ligament–bone complex. Med. Eng. Phys. 21, 95–
480 100. https://doi.org/10.1016/S1350-4533(99)00028-4
481 Provenzano, P.P., Heisey, D., Hayashi, K., Lakes, R., Vanderby R., Jr., 2002. Subfailure
482 damage in ligament: A structural and cellular evaluation. J. Appl. Physiol. 92, 362–
483 371.
484 Readioff, R., 2017. Viscoelastic Behaviour of the Canine Cranial Cruciate Ligament
485 Complex. University of Liverpool.
486 Readioff, R., Geraghty, B., Comerford, E., Elsheikh, A., 2020. A full-field 3D digital image
487 correlation and modelling technique to characterise anterior cruciate ligament
488 mechanics ex vivo. Acta Biomater. 113, 417–428.
489 https://doi.org/10.1016/j.actbio.2020.07.003
490 Ristaniemi, A., Stenroth, L., Mikkonen, S., Korhonen, R.K., 2018. Comparison of elastic,
491 viscoelastic and failure tensile material properties of knee ligaments and patellar
492 tendon. J. Biomech. 79, 31–38. https://doi.org/10.1016/j.jbiomech.2018.07.031
493 Robinson, P.S., Lin, T.W., Reynolds, P.R., Derwin, K.A., Iozzo, R. V, Soslowsky, L.J., 2004.
494 Strain-rate sensitive mechanical properties of tendon fascicles from mice with
495 genetically engineered alterations in collagen and decorin. J. Biomech. Eng. 126,
496 252–257.
497 Rosario, M.V., Roberts, T.J., 2020. Loading Rate Has Little Influence on Tendon Fascicle
498 Mechanics. Front. Physiol. 11. https://doi.org/10.3389/fphys.2020.00255
499 Savelberg, H.H.C.M., Kooloos, J.G.M., Huiskes, R., Kauer, J.M.G., 1993. An Indirect
500 Method to Assess Wrist Ligament Forces with Particular Regard to the Effect of
501 Preconditioning. J. Biomech. 26, 1347–1351. https://doi.org/Doi 10.1016/0021-
502 9290(93)90358-L

503 Slatter, D.H., 2002. Textbook of small animal surgery, 3rd ed. Saunders, Philadelphia.
504 Tanegashima, K., Edamura, K., Akita, Y., Yamazaki, A., Yasukawa, S., Seki, M., Asano, K.,
505 Nakayama, T., Katsura, T., Hayashi, K., 2019. Functional Anatomy of the
506 Craniomedial and Caudolateral Bundles of the Cranial Cruciate Ligament in Beagle
507 Dogs. Vet. Comp. Orthop. Traumatol. VCOT 32, 182–191. https://doi.org/10.1055/s-
508 0039-1678711
509 van Dommelen, J.A.W., Ivarsson, B.J., Jolandan, M.M., Millington, S.A., Raut, M., Kerrigan,
510 J.R., Crandall, J.R., Diduch, D.R., 2005. Characterization of the Rate-Dependent
511 Mechanical Properties and Failure of Human Knee Ligaments. SAE Trans. 114, 80–
512 90.
513 Vasseur, P.B., Stevenson, S., Gregory, C.R., Rodrigo, J.J., Pauli, S., Heitter, D., Sharkey, N.,
514 1991. Anterior cruciate ligament allograft transplantation in dogs. Clin. Orthop. 295–
515 304.
516 Viidik, A., 1968. Elasticity and tensile strength of anterior cruciate ligament in rabbits as
517 influenced by training. Acta Physiol. Scand. 74, 372–380. https://doi.org/DOI
518 10.1111/j.1748-1716.1968.tb04245.x
519 Wilke, V.L., Robinson, D.A., Evans, R.B., Rothschild, M.F., Conzemius, M.G., 2005.
520 Estimate of the annual economic impact of treatment of cranial cruciate ligament
521 injury in dogs in the United States. J. Am. Vet. Med. Assoc. 227, 1604–1607.
522 Wingfield, C., Amis, A.A., Stead, A.C., Law, H.T., 2000. Comparison of the biomechanical
523 properties of rottweiler and racing greyhound cranial cruciate ligaments. J. Small
524 Anim. Pract. 41, 303–307. https://doi.org/DOI 10.1111/j.1748-5827.2000.tb03206.x
525 Woo, S.L., Orlando, C.A., Camp, J.F., Akeson, W.H., 1986. Effects of postmortem storage
526 by freezing on ligament tensile behavior. J. Biomech. 19, 399–404.

527 Woo, S.L.Y., Gomez, M.A., Akeson, W.H., 1981. The time and history-dependent
528 viscoelastic properties of the canine medical collateral ligament. J. Biomech. Eng.
529 103, 293–298.
530 Woo, S.L.Y., Hollis, J.M., Adams, D.J., Lyon, R.M., Takai, S., 1991. Tensile properties of
531 the human femur-anterior cruciate ligament-tibia complex. The effects of specimen
532 age and orientation. Am. J. Sports Med. 19, 217–225.
533 Woo, S.L.Y., Ohland, K.J., Weiss, J.A., 1990a. Aging and sex-related changes in the
534 biomechanical properties of the rabbit medial collateral ligament. Mech. Ageing Dev.
535 56, 129–142.
536 Woo, S.L.Y., Peterson, R.H., Ohland, K.J., Sites, T.J., Danto, M.I., 1990b. The effects of
537 strain rate on the properties of the medial collateral ligament in skeletally immature
538 and mature rabbits: a biomechanical and histological study. J. Orthop. Res. 8, 712–
539 721. https://doi.org/10.1002/jor.1100080513
540 Zuskov, A., Freedman, B.R., Gordon, J.A., Sarver, J.J., Buckley, M.R., Soslowsky, L.J.,
541 2020. Tendon Biomechanics and Crimp Properties Following Fatigue Loading Are
542 Influenced by Tendon Type and Age in Mice. J. Orthop. Res. Off. Publ. Orthop. Res.
543 Soc. 38, 36–42. https://doi.org/10.1002/jor.24407
544

Figure 1: The extracted cranial cruciate ligaments (CCL) consisted of approximately 10 mm of the femoral and tibial bones forming femur-CCL-tibia complex. Two 1.1 mm arthrodesis wires were drilled through the bones to facilitate clamping of the sample.

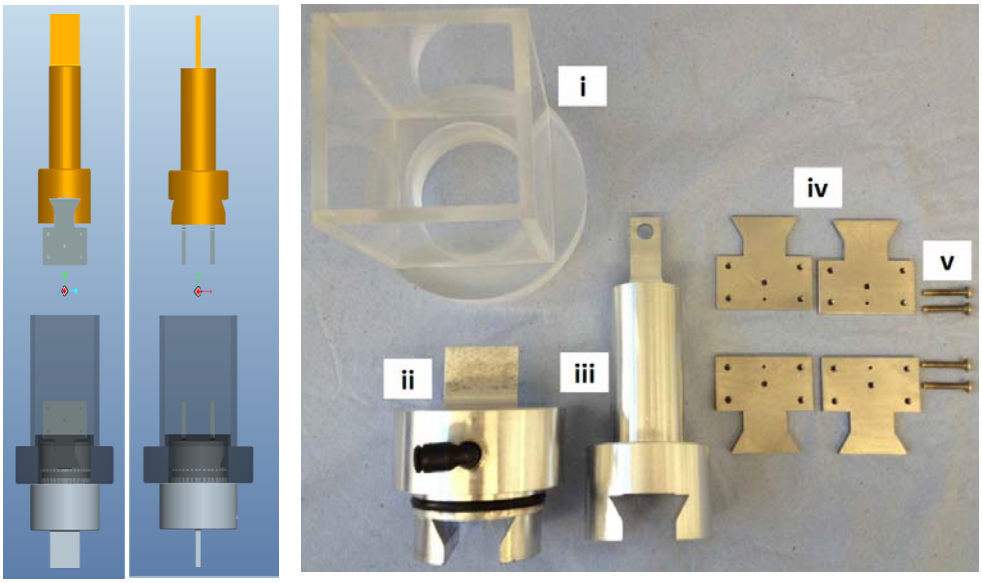

(a) **(b)**

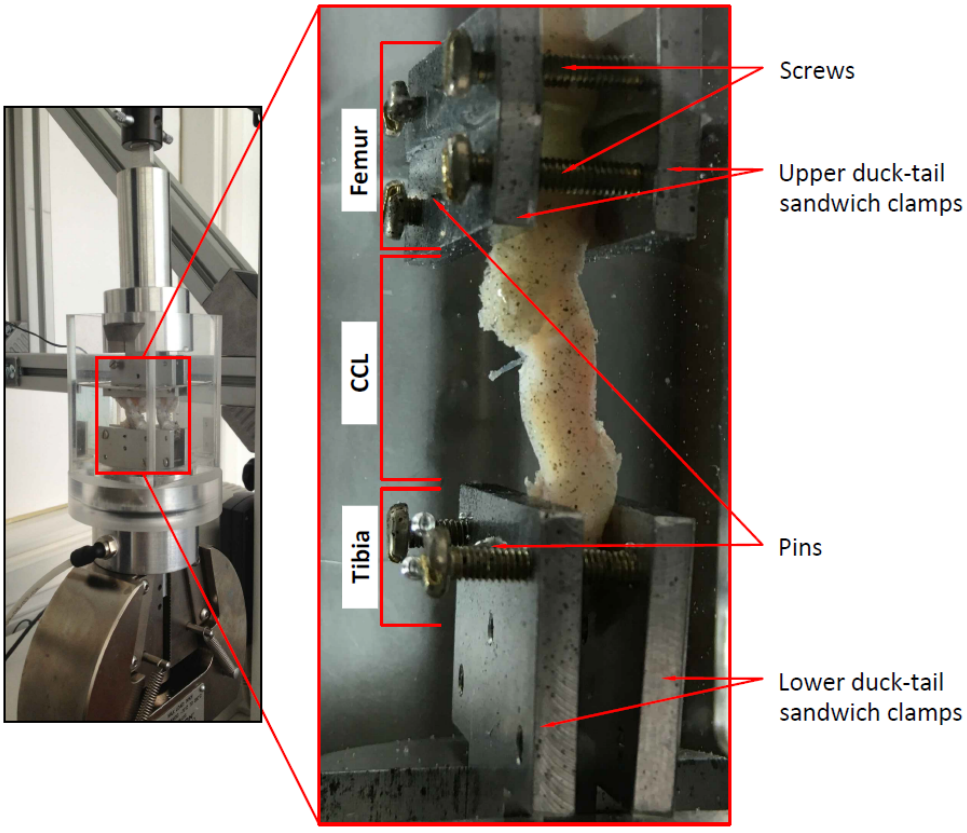

(c)

Figure 2: The experimental test setup, with (a) showing the design of the custom-made clamps that was used for (b) manufacturing the parts of the experimental testing rig. The

custom-built clamps included a (i) cylindrical Perspex tank, (ii) lower and (iii) top grips, (iv) duck-tail sandwich clamps and (v) screws. (c) An example of a cranial cruciate ligament (CCL) clamped and placed in the Perspex tank.

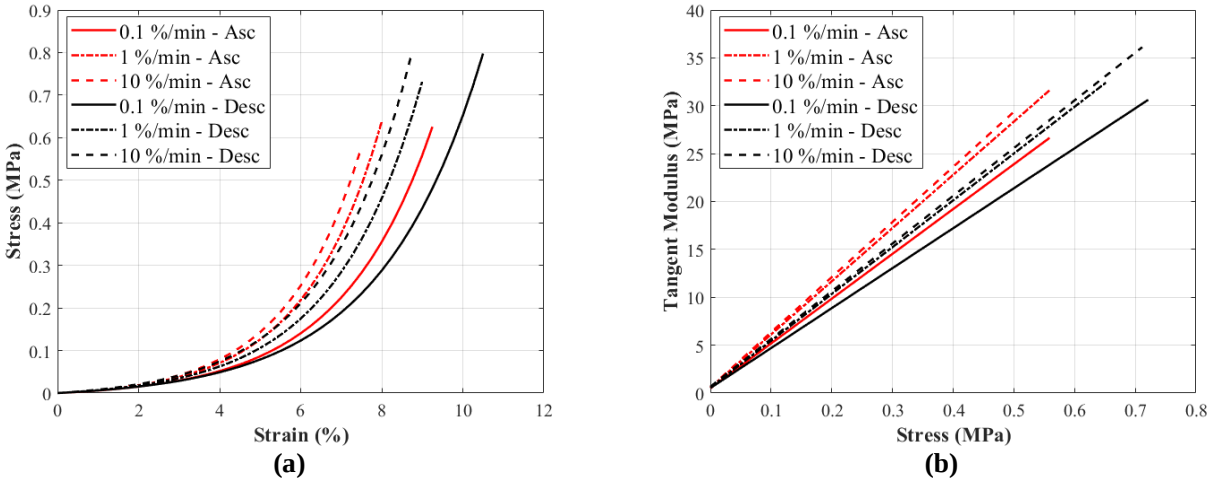

Figure 3: A typical (a) stress-strain and (b) tangent modulus-stress behaviour of a canine cranial cruciate ligament (CCL) at varying strain rates. The tensile characteristics of the CCLs was investigated following ascending (Asc) and descending (Desc) protocols at 0.1, 1 and 10 %/min strain rates.

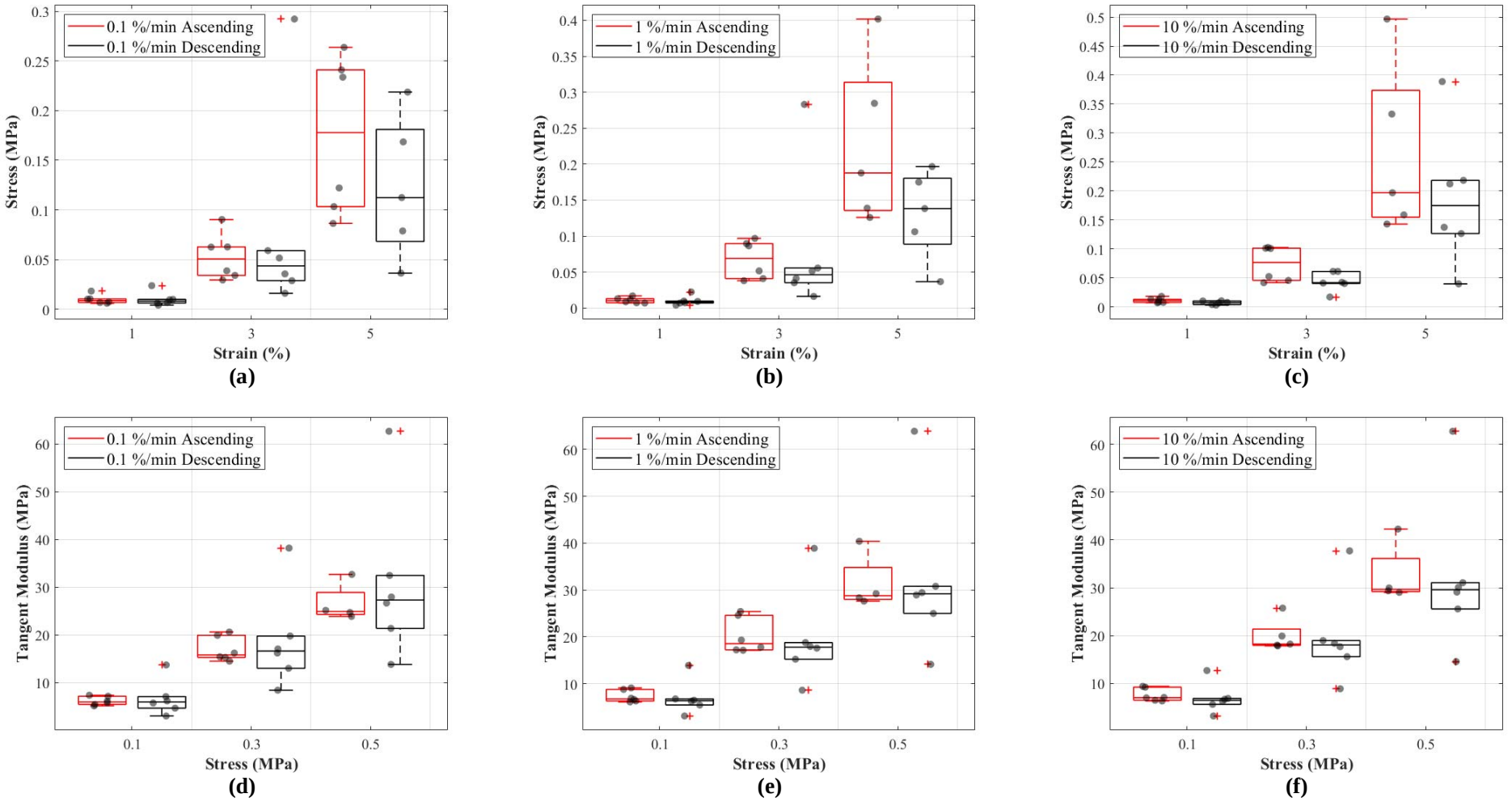

Figure 4: Tensile behaviour of the canine cranial cruciate ligaments was investigated following ascending (red line) and descending (black line) protocols at varying strain rates. The box plots show specimen variation, stress at 1, 3 and 5% strain during loading at (a) 0.1 %/min, (b) 1 %/min and (c) 10 %/min strain rates, and tangent modulus at 0.1, 0.3 and 0.5 MPa stress during loading at (d) 0.1 %/min, (e) 1 %/min and (f) 10 %/min strain rates. The outliers are indicated with a red plus sign.

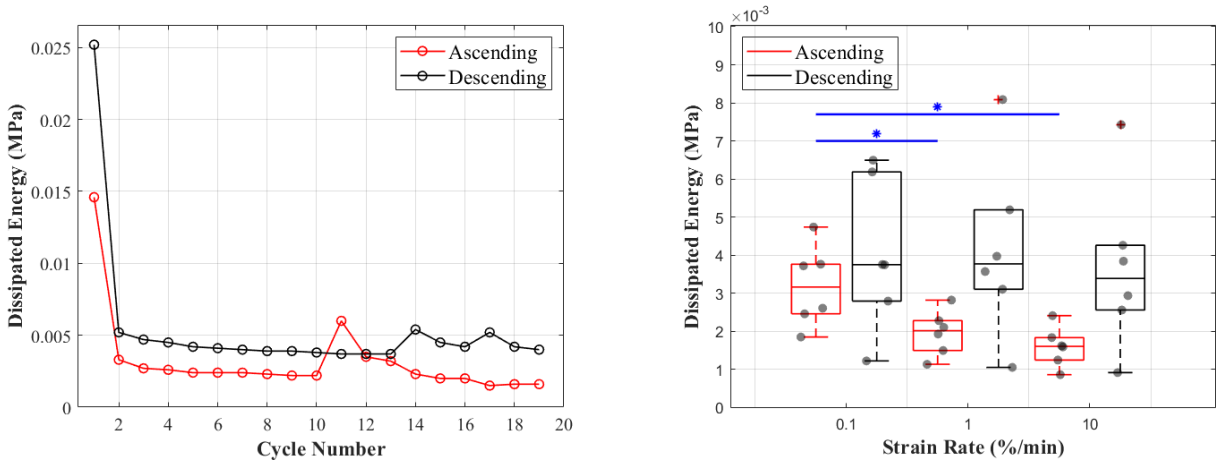

Figure 5: Dissipated energy of the canine cranial cruciate ligaments (CCL) during cyclic loading at varying strain rates. (a) This figure shows the decrease in mean dissipated energy with increasing cycles of loads. The first ten cycles represent dissipated energy during the precondition stage of the CCLs. From cycles 11 to 19 dissipated energy values are associated with CCLs during tensile tests at three different strain rates (0.1, 1 and 10 %/min with each test repeated three times). The ascending testing protocol (red line) resulted in a slightly lower dissipated energy compared to the descending (black line) testing protocol. (b) This figure shows variations in dissipated energy within the specimens. The median values (indicated by the horizontal line inside the boxes) show a decrease in dissipated energy (hysteresis) with increasing strain rates. However, this observation was only statistically significant (blue line and *) between tensile tests at strain rates of 0.1 and 1 %/min, and 0.1 and 10 %/min.

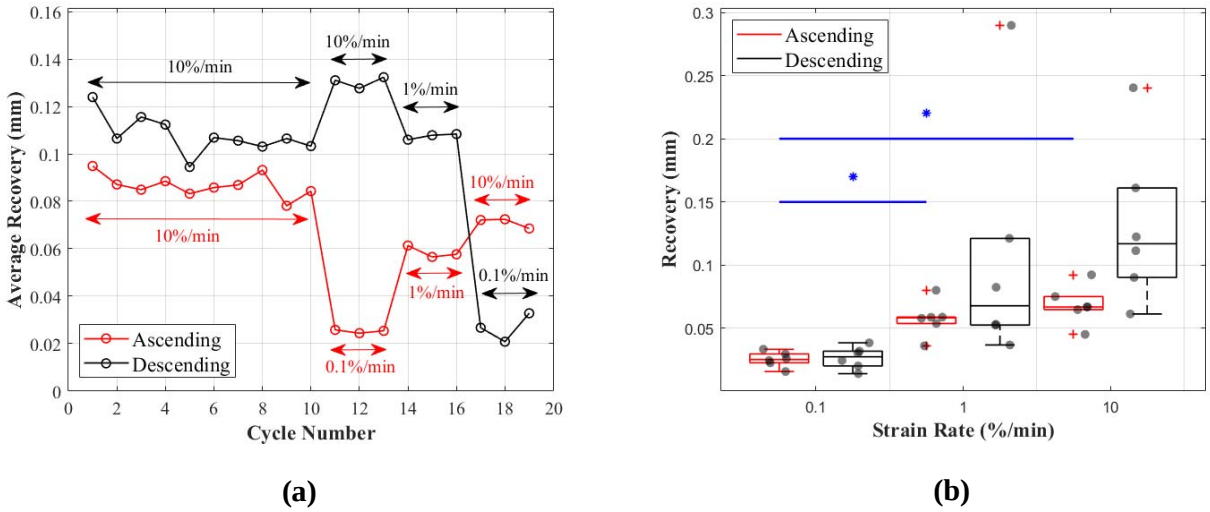

(a) **(b)**

Figure 6: Recovery of the canine cranial cruciate ligaments (CCL) during cyclic loading at varying strain rates. (a) This figure shows the average recovered length of the CCLs at different cycles. During the preconditioning cycles (the first ten cycles) recovered lengths of the ligaments are similar. Cycles associated with mechanical tests (cycles 11 to 19) for both testing protocols (ascending in red and descending in black) showed an increase in recovery with increasing strain rates. (b) This figure shows variations in length recovery within the CCLs. The box plots show an increase in recovery with increasing strain rates. This characteristic was statistically significant between tensile tests at strain rates of 0.1 and 1 %/min, and 0.1 and 10 %/min as indicated by the blue * and line.

Table 1:

The measured length of cranial cruciate ligaments (CCL) at different measurement planes (cranial, caudal, medial and lateral) for CCLs in paired canine stifle joints (n=6 pairs).

No.	Cranial Plane (mm)		Caudal Plane (mm)		Medial Plane (mm)		Lateral Plane (mm)		Average ± SD (mm)	
	Right	**Left**	**Right**	**Left**	**Right**	**Left**	**Right**	**Left**	**Right**	**Left**
1	13.51	14.54	7.88	8.16	11.76	14.10	11.00	12.31	11.04 ± 2.35	12.28 ± 2.91
2	22.79	22.07	11.20	12.00	17.00	13.1	20.54	16.93	17.88 ± 5.05	16.03±4.55
3	22.14	22.22	10.21	9.78	17.5	20.36	20.83	19.71	17.67 ± 5.34	18.02 ± 5.59
4	21.44	23.16	13.53	11.55	17.51	19.05	16.05	14.37	17.13 ± 3.31	17.033 ± 5.12
5	17.88	18.58	10.37	13.02	13.94	15.12	16.51	16.82	14.68 ± 3.30	15.89 ± 2.38
6	15.30	17.83	9.20	9.38	13.50	15.81	13.1	12.31	12.78 ± 2.57	13.83 ± 3.74
Mean ± SD (mm)	19.29 ± 3.47		10.5 2± 1.79		15.73 ± 2.60		15.87 ± 3.34			
Coefficient of Variation (%)	18.0		17.0		16.5		21.0			

Table 2:

The cross-sectional areas of cranial cruciate ligaments (CCL) for CCLs in paired canine stifle joints (n=6 pairs).

No.	**Cross-sectional area (mm^2)**	
	Right CCL	**Left CCL**
1	12.58	14.99
2	14.39	14.41
3	11.09	29.08
4	15.48	13.98
5	12.91	15.69
6	14.93	23.62
Mean ± SD (mm^2)	16.10 ± 5.10	
Coefficient of Variation (%)	31.7	